Electronic Structure and Normal Vibrations of $CH_3(OCH_2CH_2)_nOCH_3-M^+-CF_3SO_3^-$ (n = 2−4, M = Li, Na, and K)

Trupta V. Kaulgud, Nilesh R. Dhumal, and Shridhar P. Gejji*

Department of Chemistry, University of Pune, Pune 411007, India

Received: April 20, 2006

Electronic structure and the vibrational frequencies of $CH_3(OCH_2CH_2)_nOCH_3-M^+-CF_3SO_3^-$ (n = 2−4, M = Li, Na, and K) complexes have been derived from ab initio Hartree−Fock calculations. The metal ion shows varying coordination from 5 to 7 in these complexes. In tetraglyme−lithium triflate, Li^+ binds to one of the oxygens of $CF_3SO_3^-$ (triflate or Tf^-) unlike for potassium or sodium ions, which possess bidentate coordination. Structures of glyme−MTf complexes thus derived agree well with those determined from X-ray diffraction experiments. The metal ion binds more strongly to ether oxygens of tetraglyme than its di- or triglyme analogues and engenders contraction of SO (for oxygens binding to metal ion) bonds with consequent frequency upshift for the corresponding vibration in the complex relative to those in the free MTf ion pairs. Complexation of the diglyme with LiTf engenders the largest downshift (91 cm^{-1}) for the SO_2 stretching vibration of the free anion, which suggests stronger binding of lithium to the diglyme than the tri- (79 cm^{-1}) or tetraglyme (70 cm^{-1}). A frequency shift in the opposite direction for the SO (where oxygens do not coordinate to the metal) and CF_3 stretchings, which stems from the ion−polymer and anion−ion interactions, has been noticed. These frequency shifts have been analyzed using natural bond orbital analysis and difference electron density maps coupled with molecular electron density topography.

1. Introduction

Salts of weakly coordinating anions, for example, $CF_3SO_3^-$ (triflate or Tf^-) or $(CF_3SO_2)_2N^-$ (TFSI), may be dissolved in poly(ethylene oxide) (PEO) $(CH_2CH_2O)_n$ to yield solid polymer electrolytes, which have been of considerable interest in the recent years owing to their potential applications in high-energy density batteries, fuel cells, and other electrochemical devices.[1] These new salts are economical, stable, and provide a large number of fast moving charge carriers to meet the demand of ionic conductivity. Ion−polymer and ion−ion interactions in these materials are believed to play an important role in governing the ion transport phenomenon underlying the high conductivity. Cation−polymer interactions, polymer segmental motion, and ionic association (presence of ion pairs, ion triplets, or higher aggregates) are some of the important factors governing the ionic conductivity of these polymer electrolytes. With this view, how the metal ion interacts with methyl end capped PEO oligomer chains, generally referred to as "glymes", and with the anion, has been the focus of attention in the recent literature.[2,3] Molecular dynamics simulations and the ab initio molecular orbital or density functional calculations provide a direct means to analyze and understand the polymer−ion interactions which influence the conformational dynamics in the electrolytes containing alkali (Li, Na, K) and alkaline (Mg, Ca) metals complexed with PEO oligomers.[4−7] Electronic structure and vibrational frequencies of isolated $CF_3SO_3^-$ and its lithium ion pairs and higher aggregates have been studied in detail.[8−10] Analyses of normal vibrations have shown that the symmetric SO_3 stretching vibration of the free anion can be used as a probe to distinguish the ion pairs with different coordinating environments. Measured spectra of alkali metal (Li or Na) triflates have shown that ν_s (SO_3) and δ_s (CF_3) modes are influenced significantly by coordination to the metal ion. Raman and IR spectra display multiple bands for the SO_3 and CF_3 vibrations.[11,12] Vibrational spectra of AgTf, NH_4Tf, and $[Bu_4N]$Tf ion pairs reveal that the SO_3 and the CF_3 vibrations are sensitive to the potential energy environments[13] and the asymmetric SO_3 stretching vibration in different ion pairs are identified in the range 1251−1285 cm^{-1}. The CF_3 stretching are assigned to bands appearing in the region 1149−1188 cm^{-1}. For the measured spectra, the triflate anion in $(Bu_4N)Tf^-$ has been described as a "free anion" since the bulky nature of the cation is assumed to minimize cation−triflate interactions, and the SO_3 and CF_3 stretchings in this are assigned to bands at 1273 and 1149 cm^{-1}, respectively. To understand both ether oxygen−metal and ion−ion interactions in modeled ethylene glycol−M^+-X^- complexes, ab initio molecular orbital calculations have been utilized. The bond distances in these electrolytes are long in their free state,[14] and thus, the metal ion binds more strongly to polyether oxygens than the counteranion. Consequent cation−diglyme and cation−anion interactions and the IR and Raman spectra of $CH_3(OCH_2CH_2)_2OCH_3-M^+-X^-$ (M = Li, Na, and K) (X = CF_3SO_3, PF_6, $(CF_3SO_2)_2N$, ClO_4, BF_4, and SCN) have also been studied in the literature.[15,16] Crystalline phases of $CH_3(OCH_2CH_2)_nOCH_3-NaCF_3SO_3$ (n = 1, 2, and 4) have been characterized using DSC, X-ray diffraction, and IR spectroscopy.[17] It has been shown that the coordination number of Na^+ ion changes (5−7) for varying contributions from ether and anionic oxygens. Increasing the number of ethylene oxide units in the oligomer facilitates a higher coordination number for the metal. In tetraglyme−MTf (M = Li, Na) complexes, lithium binds to only one of the oxygens of the anion[7] whereas coordination via two oxygens of the SO_3 end of the anion was observed for the tetraglyme−NaTf complex. Ionic association, particularly its dependence on the

* To whom correspondence should be addressed. E-mail: spgejji@chem.unipune.ernet.in. Fax: +91-20-25691728.

10.1021/jp062431v CCC: $33.50
Published on Web 06/29/2006

TABLE 1: Comparison of Selected HF, B3LYP, and Experimental Bond Distances (in angstroms) of Diglyme−Litf and Tetraglyme −Li−Tf Complexes

(a) Diglyme−Li−Tf

	HF/6-31G**	B3LYP/6-31G**	expt
SO*	1.458	1.499	1.441
SO*	1.457	1.498	1.439
SO	1.428	1.462	1.428
CF	1.322	1.357	1.323
CF	1.312	1.337	1.310
CF	1.312	1.337	1.309
M−O	2.321	2.330	
M−O	2.340	2.307	

(b) Tetraglyme −Li−Tf

	HF/6-31G**	B3LYP/6-31G**	expt
SO*	1.458	1.500	1.435
SO*	1.451	1.491	1.432
SO	1.431	1.466	1.427
CF	1.321	1.351	1.333
CF	1.314	1.340	1.333
CF	1.314	1.339	1.330
M−O	2.500	2.456	
M−O	2.411	2.392	2.403

chain length and end group(s) in PEO−KTf, have also been studied.

In the present work, we investigate the electronic structure and the characteristic normal vibrations in the $CH_3(OCH_2CH_2)_n$-$OCH_3-M^+-CF_3SO_3^-$ ($n = 2-4$, M = Li, Na, and K) systems using the ab initio quantum chemical calculations with particular attention to how the PEO−anion and anion−cation interactions manifest in the direction of frequency shifts of SO_2 and CF_3 stretching vibrations. Natural bond orbital (NBO) analysis and molecular electron density (MED) topography coupled with different electron density maps have been used to gain insights into the reorganization of electron density consequent to these molecular interactions.

2. Computational Method

Geometry optimizations using the restricted Hartree−Fock (RHF) and the hybrid density functional theory incorporating Becke's three-parameter exchange with Lee, Yang, and Parr's (B3LYP) correlation functional[18,19] are performed on the $CH_3(OCH_2CH_2)_nOCH_3-M^+-CF_3SO_3^-$, $n = 2-4$, (M = Li, Na, and K) systems using the GAUSSIAN03 program[20] by employing the internally stored 6-31G(d, p) basis set. Stationary point geometries obtained were characterized as the saddle points or local minima on the potential energy surface by examining the number of imaginary frequencies and the eigenvalues of the Hessian matrix. Normal vibrations were assigned by visualizing the displacements of atoms around their equilibrium (mean) positions.[21] In Table 1, the anionic bond distances from the HF and B3LYP methods in the diglyme− and tetraglyme−NaTf complexes are compared with those determined from the X-ray diffraction experiment. HF/6-31G** geometrical parameters agree better with the corresponding experimental values and, hence, use of this level of theory can be justified. NBO analysis were performed subsequently.[22] MED topography[23] and different types of nondegenerate critical points (CPs) of rank 3 are identified in three-dimensional space. These include (3, −3) maxima (e.g., nuclear position), (3, +3) minima generally known as cage critical points (ccp), and saddle points denoted by (3, −1) and (3, +1), referred to as the bond critical point (bcp) and ring critical point (rcp), respectively. The difference electron density ($\Delta\rho$) was calculated by subtracting the sum of electron densities of the individual fragments from the electron density of the corresponding $CH_3(OCH_2CH_2)_n$-$OCH_3-M^+-CF_3SO_3^-$ ($n = 2-4$, M = Li, Na, and K) complex. Difference electron density maps showing contours are depicted in Figure 2 along with the bcp for different bonds in the complex.

3. Results and Discussion

In the crystalline phase of PEO, all trans conformations around the C−O and C−C are of minor importance.[24] We, therefore, consider the PEO oligomers possessing the gauche conformation around the C−C bonds of the central CH_2-CH_2-O fragment as a reference. In the following, we report the results of geometrical parameters and the vibrational spectra within the framework of the HF/6-31G** theory. Optimized geometries of $CH_3(OCH_2CH_2)_nOCH_3-M^+-CF_3SO_3^-$ ($n = 2-4$, M = Li, Na, and K) are displayed in Figure 1 along with the atomic labels used, and some of the geometrical parameters are reported in Table 2. In the triglyme−Li−Tf complex, the C−O−C bonds of the polyether linkage are elongated from 0.005−0.016 Å, relative to the corresponding distances in the T_1 conformer.

On the other hand, in the Na^+ and K^+ analogues, the C−O bond distances attached to the methyl/methoxy group are elongated by 0.017 Å. Thus, weakening of the C−O−C bonds of the oligomer backbone, which mimic the environment in the PEO, has been larger in the glyme−LiTf complex than its Na or K analogues. In other words, the Li^+−ether oxygen interactions are expected to bring about a large conformational change for the polyether linkage of the glyme. Bond angles are less sensitive to the metal−ion interaction and a maximum deviation of 5° for the C−O−C bond angle has been noticed.

As far as the Tf^- in the complexes is concerned, for the tetraglyme−LiTf complex the shortest O−M distance turns out to be 2.039 Å. The free lithium triflate ion pair yields S−O bond distances to be 1.471 Å. Shortening of SO bonds in these complexes can qualitatively be correlated to the strength of metal−anion interactions. The SO* (O* represent oxygen atoms binding to metal ion) bond distances in LiTf−tetraglyme are 0.007 Å compared with 0.006 Å for NaTf−tetraglyme and 0.003 Å for KTf−tetraglyme. It may, therefore, be inferred that binding of Li^+ to glyme has been favored over NaTf or KTf containing electrolytes. Similar inferences can be drawn in the case of diglyme− and triglyme−MTf complexes.

The metal ion in the diglyme−M−Tf complex shows pentadentate coordination binding to three oxygens of diglyme and two oxygens from the triflate. This has also been observed in the crystal structure of diglyme−$LiCF_3SO_3$.[25−28] With an increasing number of ethylene oxide units from di- to tetraglyme, Na^+ and K^+ ions exhibit an increase of coordination number from 5 to 7 and the metal ion possesses the bidentate coordination with the anion in each case. In the X-ray determined crystal structure of tetraglyme−LiTf, unlike that for the sodium or potassium triflate complexes, the metal ion shows monodentate coordination with the anion and facilitates the Li^+ to bridge between different CF_3SO_3 ions in electrolytes.[7] The HF/6-31G** derived structure of the tetraglyme−Li−Tf complex supports these inferences. A higher coordination number has been noted with increased chain length of the oligomer.

As pointed out earlier, the interaction of ether oxygens to the metal ion brings about a conformational change in its backbone which manifests in their vibrational spectra.[29,30] HF/6-31G(d,p) vibrational frequencies (scaled by 0.89) of $CH_3(OCH_2CH_2)_nOCH_3-M^+-CF_3SO_3^-$ ($n = 2-4$, M = Li, Na,

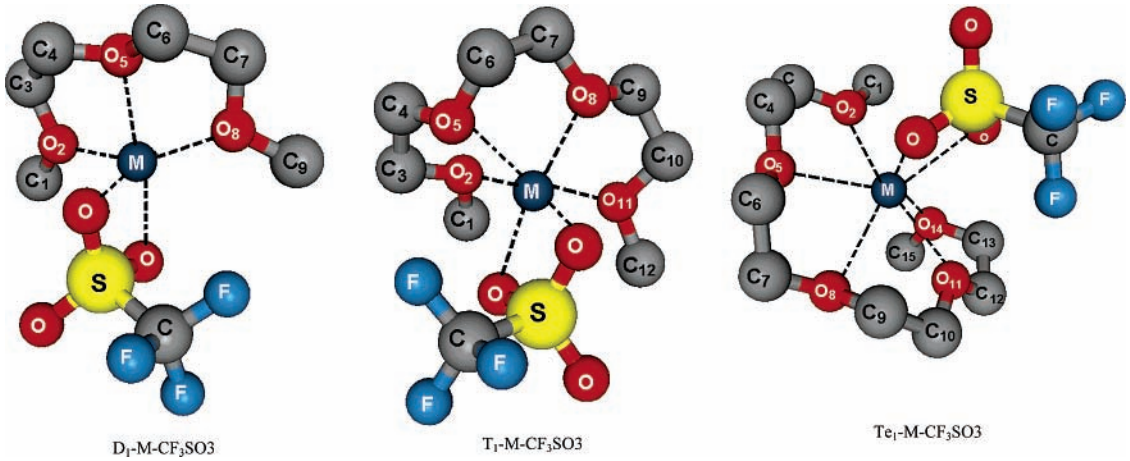

Figure 1. Optimized geometries of $CH_3(OCH_2CH_2)_nOCH_3-M^+-CF_3SO_3^-$ ($n = 2-4$, M = Li, Na, and K). Hydrogens are omitted for clarity.

TABLE 2: Selected Optimized Geometrical Parameters (bond lengths in angstroms and bond angles in degrees) of Free Diglyme (D_1), Triglyme (T_1), Tetraglyme (Te_1), and Their Complexes with $M^+-CF_3SO_3^-$ (M = Li, Na, and K)

		$D_1-M-CF_3SO_3$				$T_1-M-CF_3SO_3$				$Te_1-M-CF_3SO_3$		
	D_1	Li	Na	K	T_1	Li	Na	K	Te_1	Li	Na	K
C_1-O_2	1.391	1.405	1.409	1.407	1.391	1.410	1.410	1.409	1.397	1.401	1.402	1.398
O_2-C_3	1.392	1.401	1.400	1.397	1.392	1.400	1.399	1.395	1.392	1.411	1.398	1.407
C_3-C_4	1.510	1.514	1.511	1.511	1.511	1.511	1.511	1.511	1.517	1.575	1.511	1.517
C_4-O_5	1.393	1.404	1.401	1.402	1.393	1.399	1.401	1.403	1.401	1.394	1.404	1.397
O_5-C_6	1.393	1.405	1.403	1.401	1.393	1.398	1.397	1.399	1.393	1.395	1.403	1.397
C_6-C_7	1.510	1.514	1.511	1.511	1.517	1.518	1.517	1.516	1.516	1.514	1.514	1.511
C_7-O_8	1.392	1.400	1.399	1.398	1.396	1.404	1.404	1.402	1.400	1.409	1.402	1.406
O_8-C_9	1.391	1.406	1.411	1.406	1.395	1.403	1.402	1.403	1.397	1.400	1.405	1.403
C_9-C_{10}					1.510	1.510	1.510	1.511	1.517	1.510	1.511	1.515
$C_{10}-O_{11}$					1.392	1.402	1.399	1.395	1.395	1.405	1.398	1.404
$O_{11}-C_{12}$					1.391	1.407	1.408	1.408	1.395	1.410	1.397	1.403
$C_{12}-C_{13}$									1.510	1.511	1.518	1.510
$C_{13}-O_{14}$									1.393	1.394	1.407	1.401
$O_{14}-C_{15}$									1.393	1.402	1.399	1.399
O_2-M		2.039	2.367	2.771		2.192	2.447	2.810		2.070	2.371	2.895
O_5-M		2.101	2.367	2.856		2.107	2.406	2.871		3.294	2.552	2.762
O_8-M		2.059	2.387	2.771		2.175	2.442	2.862		2.162	2.712	2.986
$O_{11}-M$						2.205	2.439	2.794		2.184	2.412	2.885
$O_{14}-M$										2.163	2.487	2.802
$C_1-O_2-C_3-C_4$	158	−174	−174	−175	172	−180	175	175	−75	165	−163	−171
$O_2-C_3-C_4-O_5$	45	−53	−58	−65	−75	57	62	65	−72	53	−58	−64
$C_3-C_4-O_5-C_6$	−174	171	176	−178	167	−179	−177	−180	−177	−172	176	−175
$C_4-O_5-C_6-C_7$	174	−171	−172	−177	−91	173	178	−178	−84	169	179	−179
$O_5-C_6-C_7-O_8$	−45	51	61	−61	−72	−53	−55	−62	80	−58	60	67
$C_6-C_7-O_8-C_9$	−158	171	178	152	177	−85	−86	−85	171	−159	89	85
$C_7-O_8-C_9-C_{10}$					−180	155	172	−176	87	−97	173	169
$O_8-C_9-C_{10}-O_{11}$					73	−59	−63	−64	82	−72	60	63
$C_9-C_{10}-O_{11}-C_{12}$					−175	−176	−176	−177	170	142	−167	176
$C_{10}-O_{11}-C_{12}-C_{13}$									−173	−124	172	180
$O_{11}-C_{12}-C_{13}-O_{14}$									−81	65	−54	−60
$C_{12}-C_{13}-O_{14}-C_{15}$									176	89	−80	−84

and K) and the corresponding glymes are given Table 3. Some of the frequencies of normal vibrations from the observed spectra are also given. Assigning normal vibrations in the measured spectra is relatively difficult. A correlation of these bands with the theoretically calculated harmonic vibrational frequencies has proven useful in understanding the metal ion induced spectral changes of the oligomer.[31] It may be noticed from Table 3a that the CH_2 rocking vibrations near 1370 and 1354 cm^{-1} in the observed spectra correspond to the 1376 and 1352 cm^{-1} doublet in the calculated spectra. These vibrations get more separated (24 cm^{-1}) upon metal ion coordination. Similarly, the CH_2 wag vibrations in the diglyme were observed at 874 and 855 cm^{-1} (a separation of 19 cm^{-1}) and a downshift for the latter to 836 cm^{-1} leads to separation nearly twice as large upon metal ion coordination. HF calculated CH_2 rocking vibrations (1381 and 1356 cm^{-1}) in free diglyme conformer are insensitive to coordination to the metal ion. It should be noted here that, in electrolytes comprised of diglyme and alkali metal triflates, the metal coordinates to three oxygens of the diglyme and two from the anion and exhibits pentadentate coordination. Metal ion induced conformational change of diglyme manifests in its vibrational spectra particularly in the 862 and 839 cm^{-1} vibrations of free diglyme, which are assigned to the CH_2 wag. A separation of these bands becomes nearly twice as large upon complexation with LiTf, which has also been observed in the measured spectra. In the diglyme−NaTf and diglyme−KTf complexes, this separation amounts to ∼32 cm^{-1}. The intense C−O−C stretching vibration 1138 cm^{-1} in the HF calculations has been noted only in case of the free diglyme. This vibration could not be correlated with any of the vibrations in the experimental spectra.

Selected HF vibrational frequencies of triglyme and triglyme−MCF_3SO_3 (M = Li, Na, and K) have been presented in Table 3b. Measured spectra of the triglyme−$LiCF_3SO_3$

TABLE 3: Selected HF Vibrational Frequencies (in cm^{-1}) of $CH_3-(O-CH_2-CH_2-)_2O-CH_3$ and Its MCF_3SO_3 (M = Li, Na, and K) Complexes[a]

	(a) $D_1-M-CF_3SO_3$				expt	
	D_1	Li	Na	K	D_1	$D_1-Li-Tf$
CH_2 scissor	1457 (12)	1455 (14)	1455 (12)	1456 (13)		1460
	1454 (13)	1453 (10)	1454 (14)	1445 (11)	1453	
CH_2 rock	1431 (21)					
	1381 (44)	1379 (36)	1377 (32)	1382 (36)	1370	1376
	1356 (122)	1352 (77)	1352 (92)	1356 (95)	1354	1352
CH_2 twist	1279 (32)	1253 *17)	1270 (15)	1277 (32)		
			1259 (80)			
		1252 (24)	1259 (52)			
	1241 (43)	1242 (45)	1240 (50)	1243 (45)		
	1231 (18)			1241 (96)		
				1230 (18)		
				1219 (153)		
	1211 (161)	1209 (79)	1205 (73)	1209 (97)		
		1157 (21)	1156 (23)			
		1156 (41)				
COC stretch	1169 (51)					
	1160 (88)					
			1155 (52)	1155 (34)		
		1131 (507)	1125 (151)	1132 (211)		
		1110 (253)				
CH_2 wag	1151 (19)	1064 (17)				
COC stretch	1148 (74)					
	1138 (393)					
CH_2 wag	1121 (38)		1121 (127)	1118 (37)		
COC stretch			1105 (261)	1112 (368)		
CC + COC stretch	1021 (37)	1010 (24)	1010 (62)	1011 (53)		
		1008 (61)				
CH_2 wag	862 (42)	869 (37)	858 (37)	862 (46)	874	874
	839 (20)	825 (19)	827 (19)	829 (19)	855	836

	(b) $T_1-M-CF_3SO_3$				expt
	T_1	Li	Na	K	T_1-Li
CH_2 scissor					1478
					1470
	1456 (9)		1457 (10)	1458 (10)	1461
	1454 (14)	1455 (13)	1452 (11)	1455 (11)	1453
		1449 (14)	1447 (16)	1454 (12)	
				1453 (18)	
CH_2 rock	1432 (16)		1427 (10)	1430 (11)	
	1420 (14)	1425 (10)			
		1412 (10)			
	1369 (102)	1366 (80)	1367 (84)	1369 (80)	1367
	1351 (107)	1346 (46)	1348 (61)	1351 (76)	1352
					1346
					1339
CH_2 twist	1297 (38)	1284 (51)	1290 (46)	1294 (33)	
	1277 (29)	1263 (25)	1268 (24)	1274 (22)	
				1267 (20)	
	1245 (53)	1237 (20)	1239 (25)	1243 (13)	
	1232 (26)	1234 (17)	1233 (11)	1232 (23)	
		1228 (11)	1231 (12)		
	1207 (22)	1226 (84)	1203 (46)		
			1202 (30)		
COC stretch	1208 (98)				
	1174 (19)				
	1162 (72)			1162 (34)	
CH_2 wag		1203 (27)		1207 (75)	
		1202 (45)		1205 (36)	
	1155 (83)	1156 (40)	1153 (16)		
	1152 (89)				
COC stretch	1139 (102)	1146 (103)	1143 (127)	1142 (99)	
CH_2 wag		1136 (15)	1133 (13)	1132 (16)	
COC stretch	1143 (174)		1118 (369)	1124 (419)	
	1128 (135)	1113 (14)	1108 (55)	1110 (168)	
CH_2 wag		1100 (42)	1103 (26)	1100 (17)	
	1097 (24)	1083 (28)	1085 (18)		
COC stretch		1064 (33)			
CC + COC stretch	1067 (26)	1030 (37)	1066 (33)	1068 (38)	
	1043 (27)	1010 (8)	1038 (30)	1040 (23)	
	1021 (35)	1006 (46)	1013 (15)	1016 (16)	
			1007 (47)	1009 (64)	
CH_2 wag	934 (32)	920 (28)	922 (30)	925 (37)	
	902 (26)	902 (13)	902 (14)	899 (17)	
	853 (31)	858 (18)	854 (14)	855 (19)	860
					843
	835 (19)	838 (35)	838 (36)	842 (38)	833
		830 (16)	829 (17)	824 (19)	829

TABLE 3 (Continued)

		(c) $Te_1-M-CF_3SO_3$		
	Te_1	Li	Na	K
CH_2 scissor	1466 (6)	1454 (12)	1462 (10)	1459 (19)
	1456 (6)	1453 (8)	1457 (10)	1457 (8)
	1454 (7)		1455 (10)	
	1449 (8)			
CH_2 rock	1432 (12)		1434 (10)	1436 (10)
	1410 (9)			
	1402 (9)	1394 (22)		
	1374 (37)	1371 (48)	1374 (40)	1375 (29)
	1362 (123)	1359 (103)	1359 (121)	1360 (115)
	1351 (62)	1346 (26)	1348 (47)	1349 (72)
CH_2 twist	1308 (69)	1295 (58)	1294 (9)	1296 (29)
		1294 (34)	1292 (32)	
	1277 (31)	1273 (23)	1271 (52)	1278 (30)
	1249 (52)	1261 (123)	1260 (11)	1251 (19)
	1246 (19)	1257 (62)	1246 (15)	1242 (196)
	1240 (21)	1248 (48)	1240 (35)	1230 (21)
	1234 (14)	1243 (113)		
		1228 (12)		
				1207 (39)
CH_2 wag	1211 (95)	1211 (58)	1210 (50)	1207 (76)
	1208 (47)	1206 (48)	1205 (63)	1203 (150)
COC stretch	1170 (62)	1176 (213)	1169 (43)	1168 (10)
	1167 (117)	1175 (175)	1160 (45)	1156 (32)
	1154 (120)			
CH_2 wag	1153 (53)	1159 (59)	1156 (32)	1153 (30)
		1155 (25)	1151 (107)	1149 (66)
		1150 (32)	1145 (16)	1144 (36)
		1145 (52)		1139 (146)
		1138 (74)		1129 (160)
		1126 (49)		
COC stretch	1147 (145)		1142 (83)	
	1136 (140)		1127 (171)	
	1125 (140)	1114 (124)	1114 (161)	1113 (277)
CH_2 wag	1108 (13)	1102 (142)	1113 (51)	1108 (69)
	1084 (15)	1093 (51)	1097 (34)	1096 (20)
	1082 (15)			
COC stretch				1069 (24)
				1066 (18)
CC + COC stretch	1068 (32)	1075 (27)	1078 (53)	
	1041 (30)	1061 (10)	1068 (24)	
	1027 (40)	1032 (29)	1063 (12)	
	1024 (12)	1018 (14)	1028 (27)	1032 (29)
	982 (34)	1012 (52)	1016 (33)	1020 (24)
CH_2 wag		982 (76)		985 (38)
	937 (45)		927 (40)	
	925 (48)	929 (21)	918 (28)	931 (41)
	891 (15)	920 (30)		922 (33)
	854 (30)	861 (14)		895 (14)
	837 (26)	831 (13)	841 (45)	854 (13)
	826 (9)	818 (22)	825 (18)	839 (47)
		808 (23)		
		803 (17)		

[a] The infrared intensities (in km·mol^{-1}) are given in parentheses. Experimental frequencies of T_1 and its LiTf complex are also given.

complex has been presented along with the above results. As shown, the 1453 cm^{-1} vibration in the measured spectra correlates well with the HF calculations[32] (CH_2 scissor). This vibration is insensitive to the coordinating environment. A near doublet at 1369 and 1351 cm^{-1} assigned to CH_2 rocking has been noted for triglyme and also found in the triglyme−MTf complexes. Separation of these bands amounts to 21 cm^{-1} in the triglyme−M−Tf complexes. These vibrations have also been observed in the IR spectrum. As shown in Table 3b, the vibrations in the 1297−1207 cm^{-1} region are assigned to a CH_2 twist. A downshift of the CH_2 wag (934 cm^{-1}) vibration has also been noticed upon complexation with metal triflate. A near doublet, namely (853 and 835 cm^{-1}), has been predicted in the triglyme conformer. The former vibration shifts to 858 cm^{-1} in the triglyme−LiTf and can be correlated with the vibration near 860 cm^{-1} in the measured spectra. A small upshift for the 835 cm^{-1} vibration in the above doublet has also been noticed. As shown in Table 3b, the C−O−C stretchings of the triglyme bands are predicted in the 1067 and 1021 cm^{-1} regions and the latter vibration is downshifted in the complex owing to polymer−ion interactions.

Calculated frequencies of the tetraglyme and tetraglyme−M−Tf (M = Li, Na, and K) are compared in Table 3c. The following conclusions can be drawn. The CH_2 rockings of tetraglyme assigned to the 1374 and 1362 cm^{-1} vibrations can be correlated to a near doublet (a separation of ∼12−15 cm^{-1}) in the tetraglyme−MCF_3SO_3 complexes. C−O−C stretching vibrations are found in the 1170 to 1125 cm^{-1} region for the tetraglyme. The 1170 cm^{-1} vibration of the tetraglyme has been upshifted by 6 cm^{-1} for the LiTf complex and is nearly

TABLE 4: Bond Distances (in angstroms), Vibrational Frequencies, ν (in cm^{-1}), and Electron Densities, ρ (in atomic units), in Antibonding Orbitals of S−O, C−F, and O−M Bonds in Tf$^-$ (C_{3v} symmetry) and Its $CH_3(OCH_2CH_2)_2OCH_3-M^+-CF_3SO_3$ (n = 2) (M = Li, Na and K) Complex[a]

		ν	ρ		ν	ρ		ν	ρ		ν	ρ
		(a) $CF_3SO_3^-$			$D_1-Li-CF_3SO_3$			$D_1-Na-CF_3SO_3$			$D_1-K-CF_3SO_3$	
SO*	1.443	1244 (568)	0.136	1.463	1153 (277)	0.142	1.458	1162 (217)	0.141	1.455	1174 (254)	0.142
SO*			0.136	1.457		0.139	1.457		0.140	1.455		0.141
SO			0.136	1.426	1283 (506)	0.123	1.428	1279 (445)	0.125	1.427	1285 (454)	0.124
CF	1.323	1195 (78)	0.081	1.312	1250 (338)	0.079	1.312	1251 (366)	0.078	1.313	1249 (407)	0.078
CF			0.081	1.319	1223 (120)	0.083	1.322	1216 (116)	0.084	1.329	1194 (172)	0.086
CF			0.081	1.312		0.079	1.312		0.078	1.313		0.078
O−M				2.012			2.321			2.700		
O−M				2.109			2.340			2.700		
		(b) $CF_3SO_3^-$			$T_1-Li-CF_3SO_3$			$T_1-Na-CF_3SO_3$			$T_1-K-CF_3SO_3$	
SO*	1.443	1244 (568)	0.136	1.460	1165 (498)	0.141	1.457	1168 (238)	0.140	1.455	1177 (194)	0.141
SO*			0.136	1.454		0.136	1.455		0.138	1.454		0.140
SO			0.136	1.429	1277(519)	0.124	1.430	1275 (437)	0.124	1.430	1258 (245)	0.125
CF	1.323	1195 (78)	0.081	1.317	1245 (357)	0.081	1.320	1246 (251)	0.082	1.325	1247 (419)	0.085
CF			0.081	1.314	1226 (84)	0.078	1.314	1218 (106)	0.078	1.314	1203 (121)	0.078
CF			0.081	1.313		0.078	1.313		0.078	1.313		0.078
O−M				2.150			2.374			2.741		
O−M				2.109			2.368			2.711		
		(c) $CF_3SO_3^-$			$Te_1-Li-CF_3SO_3$			$Te_1-Na-CF_3SO_3$			$Te_1-K-CF_3SO_3$	
SO*	1.443	1244 (568)	0.136	1.464	1174 (175)	0.147	1.458	1175 (304)	0.141	1.456	1177 (272)	0.141
SO*			0.136	1.444		0.131	1.451		0.136	1.452		0.140
SO			0.136	1.433	1270 (335)	0.124	1.431	1273 (403)	0.124	1.430	1274 (402)	0.125
CF	1.323	1195 (78)	0.081	1.321	1241 (287)	0.082	1.321	1243 (395)	0.082	1.324	1243 (248)	0.085
CF			0.081	1.314		0.078	1.314	1214 (110)	0.078	1.315	1203 (150)	0.079
CF			0.081	1.314		0.077	1.314		0.078	1.314		0.078
O−M				1.921			2.500			2.813		
O−M							2.411			2.773		

[a] Infrared intensities (in km·mol^{-1}) are given in parentheses.

unchanged in its NaTf and KTf counterparts. The intense 1147 cm^{-1} (C−O−C stretch) vibration shows a downshift of 5 cm^{-1} for the tetraglyme−NaTf complex. Similarly, the 1108 cm^{-1} (CH_2 wag) vibration in this complex moves to higher wavenumber (1113 cm^{-1}) and shifts in the opposite direction (1102 cm^{-1}) in its LiTf analogue. This vibration remains unchanged in the case of the tetraglyme−KTf complex. The respective 1041 and 1027 cm^{-1} vibrations are assigned to C−C stretching coupled with the C−O−C stretching in tetraglyme. An increased separation of 29 cm^{-1} has been noted in the tetraglyme−LiTf complex compared with 5 cm^{-1} for NaTf and 12 cm^{-1} for KTf complexes.

Anionic vibrations in the polymer electrolytes yield insights for the ion−ion interactions and frequency shifts of characteristic vibrations can be correlated to the local structures. The vibrational frequencies of Tf$^-$ in a different environment vary from 1153 to 1285 cm^{-1} (cf. Table 4) Ion−ion interactions weaken the SO bonds in the complexes, and thus, the corresponding vibration shifts to a lower wavenumber compared with the free anion. These vibrational frequencies can qualitatively be correlated to the strength of the interactions. The diglyme−LiTf complex shows a red shift of 91 cm^{-1}. Analogously, shifts of SO_2 stretching vibrations in di-, tri-, and tetraglyme metal triflates range from 91 to 70, 79 to 67, and 70 to 67 cm^{-1}, respectively. This suggests weak M^+-Tf^- interactions in the tetraglyme complex over di- and triglymes implying stronger binding of ether oxygens of tetraglyme to MTf, which possibly renders high ionic conductivity in the tetraglyme−metal triflates. The molecular interactions bring about reorganization of electron density, which leads to a shift to higher wavenumber for stretching vibration of bonds which do not bind to the metal ion.[33] Thus, a blue shift (frequency shift to higher wavenumber) has been predicted for the SO_2 (oxygen atoms not participating in cation−anion interactions) and CF_3 stretching vibrations in the glyme−MTf complexes. Frequency shifts as large as ∼39 cm^{-1} for SO_2 stretching and 55 cm^{-1} for CF_3 stretching have been obtained in the diglyme−LiTf complex. Blue shifts of SO and CF stretching vibrations follow the trend: diglyme > triglyme > tetraglyme. These stretching frequencies thus follow in the order of the M−O bond distances given in Table 4. In other words, the strength of anion−cation interactions can be gauged from the shifts of SO and CF stretching vibrations, which stems from different potential energy environments of the anion (Tf$^-$). The inferences drawn here agree qualitatively with observed IR or Raman spectra.[30]

Both the glyme−metal ion and metal−anion interactions lead to varying bond strengths in the anionic part of the complex, which can be analyzed using the NBO analysis. Thus, the electron density in the antibonding orbitals of the CF and SO bonds in the free anion and the complexes are summarized in Table 4. An increase of electron density in the localized antibonding orbital of SO* (O* denotes oxygen atoms coordinating to metal) bonds in the anion engenders a charge transfer to the metal with a consequent bond elongation leading to a downshift in the frequency of the corresponding stretching vibration compared with the free anion. On the other hand, redistribution of electron density causes a transfer of a large portion of density to the bonds not participating in the ion−ion molecular interactions thereby increasing the bond strength and hence a concomitant frequency upshift for the corresponding stretching vibration. Thus, the blue shifts of CF_3 and SO_2 stretchings can be explained. An increased number of ethylene oxide units in the oligomer exhibit a regular trend, namely, diglyme > triglyme > tetraglyme for the blue shift of the SO stretching in the glyme−MTf (M = Li, Na) complexes. It may be remarked here that the frequency downshift of SO_2 vibration also follows the above rank order (cf. Table 4a−4c) and suggests the stronger binding for lithium toward the ether oxygens of the oligomers.

The change of metal ion from lithium to potassium brings about a frequency shift of the SO* vibration in the glyme−metal complexes. Thus, this SO_2 stretching has been downshifted

TABLE 5: Electron Density at the Bond Critical Point (ρ_{bcp}) of Different S−O, C−F, and O−M Bonds in the Anionic Part of $CH_3(OCH_2CH_2)_nOCH_3-M^+-CF_3SO_3$ ($n = 2-4$) (M = Li, Na, and K)

		$D_1-MCF_3SO_3$			$T_1-MCF_3SO_3$			$Te_1-MCF_3SO_3$		
	$CF_3SO_3^-$	Li	Na	K	Li	Na	K	Li	Na	K
SO* [a]	0.297	0.287	0.289	0.290	0.289	0.290	0.290	0.285	0.285	0.290
SO* [a]		0.294	0.290	0.290	0.292	0.291	0.291	0.297	0.293	0.292
SO		0.306	0.305	0.306	0.305	0.305	0.304	0.304	0.305	0.305
CF	0.275	0.280	0.278	0.271	0.282	0.280	0.274	0.279	0.278	0.276
CF		0.287	0.287	0.285	0.286	0.285	0.284	0.285	0.285	0.285
CF		0.287	0.287	0.285	0.286	0.286	0.285	0.285	0.285	0.286
M−O		0.018	0.019	0.018	0.016	0.018	0.016	0.028	0.013	0.014
M−O		0.023	0.021	0.018	0.017	0.018	0.017	-	0.016	0.015

[a] O* denotes the oxygen atoms interacting with the metal ion. See text for details.

by 91 cm^{-1} in the diglyme−LiTf complex compared with that of 82 cm^{-1} for $NaTf^-$ and 70 cm^{-1} for KTf. A similar trend has also been noticed for the metal triflates complexed with tri- and tetraglymes.

The MED topography has been outlined in section 2. In the following, we will discuss how it can be utilized to understand the direction of frequency shifts caused by the anion−cation molecular interactions. Electron densities at the bond critical point (ρ_{bcp}) in Tf^- in its free state and metal triflate complexes are given in Table 5. Here, ρ_{bcp} emerges as a signature of the metal ether oxygen atoms or metal anion interactions and yields a measure of the strength of molecular interactions.[34,35] Table 5 shows that ρ_{bcp} values of the CF and SO bonds in the diglyme−MTf complexes are in the range of 0.018−0.307 au. Compared with the free anion, the SO* bonds of the complexes, where O* denotes the oxygen participating in the O−M interactions, the ρ_{bcp} values are decreased. These frequency downshifts are in accordance with a decrease of corresponding ρ_{bcp} values. A blue shift of the CF_3 stretching vibration of the anion on the other hand can only be qualitatively correlated in a similar way. As may be noticed from Table 5, the weakening of SO* bonds in the polyether−MTf complexes can be seen from the ρ_{bcp} values. Accordingly, it may be expected that the corresponding SO bonds in the diglyme−LiTf are weak compared with its NaTf or KTf counterparts, and the concomitant "frequency downshift" of the corresponding stretching vibration in the complex has been predicted.

In the following, we discuss how the difference MED can be utilized to study the reorganization of electron density owing to the metal ion−oligomer and cation−anion interactions. Figure 2 displays the difference electron density contour maps of $CH_3(OCH_2CH_2)_nOCH_3-Li^+-CF_3SO_3^-$ ($n = 2-4$) in two different planes, namely, (i) a plane passing through ether oxygens of diglyme and (ii) a plane passing through all the atoms of the counteranion present in the anion−metal interactions. The $\Delta\rho$ contours in the range $\pm 0.001-0.0009$ au are displayed. The blue lines represent positive valued contours, and the negative valued contours appear in red. The zero valued contour has been depicted as a black line. Figure 2a shows the difference electron density map of diglyme−$LiCF_3SO_3$. As may be noticed, the bcp of the C−O−C bonds with the oxygen atoms interacting with the metal appear in a region (red) where the electron density is depleted. This explains the frequency downshift of the C−O−C stretching vibrations of diglyme in contrast to the C−C and C−H bonds for which the bcp emerges in a (blue) region (enhancement of electron density). This leads to an increase of bond strength of the corresponding vibration, which shifts to higher wavenumber. For anionic vibrations in these complexes, the bcp for the CF bonds appears in the blue region (bond strengthening) in contrast to the SO bonds when oxygen atoms coordinate to the metal. Reorganization of electron density, following these interactions, engenders the density bcp of the remaining SO bonds in a blue region and, therefore, leads to a frequency upshift for the corresponding stretching vibration. Thus, the direction of frequency shifts of different anionic SO_2 and CF_3 stretching vibrations can be explained.

Difference electron density contours of electrolytes comprised of triglyme and tetraglyme complexed with LiTf are depicted in parts b and c of Figure 2. As explained earlier, the bcp of the blue-shifted CF bond lies in a region (blue contours) where the electron density is increased. For the red-shifted SO bond, the bcp has been located in a region with decreased electron density (red contours). The distinction of the direction of the frequency shifts has thus been facilitated from the appearance of the bcp(s) in blue or red contour(s) regions. Here again, the fluorine atoms not interacting with a metal ion engender frequency upshift of the CF stretching vibration and thus can be distinguished from the rest.

4. Conclusions

This work presents a systematic investigation of electronic structure and vibrational spectra of $CH_3(OCH_2CH_2)_nOCH_3-M^+-CF_3SO_3^-$, $n = 2-4$, (M = Li, Na, and K). The following conclusions may be drawn: (i) Li^+ binds strongly to the central ether oxygens of the oligomer whereas Na^+ and K^+ bind to the oxygens of the terminal groups of oligomers O−M bond distances in these complexes predicting that 1:1 diglyme−cation ion pairs are favored in electrolytes containing LiTf and possibly favor a large number of charge carriers in the electrolytes than those comprised of NaTf or KTf. (ii) In the glyme−M−Tf complexes studied herein, the metal ion shows bidentate coordination with the triflate anion except for the tetraglyme−LiTf, where it binds to only one of the oxygens of the anion, which facilitates a bridge between different $CF_3SO_3^-$ anions and renders a large flexibility to the ion pair in the electrolytes. The predicted structure of the complex agrees well with those derived from the X-ray diffraction experiment. (iii) A conformational change around the C−O−C bonds of diglyme−MX systems engenders a change in the vibrational spectra. Consequently, the 1431 cm^{-1} vibration of free diglyme (assigned to CH_2 rocking) vanishes in the complex. A downshift of C−O−C stretching vibration has been correlated to the strength of metal−ether oxygen interactions. Furthermore, a near doublet (1370 and 1354 cm^{-1}) in the observed IR spectrum of diglyme becomes more separated upon coordination with Li^+. This has also been noticed from the present calculations where these vibrations correspond to 1381 and 1356 cm^{-1} in the diglyme conformer which become more separated (nearly twice as large) upon metal coordination. (iv) For triglyme, a downshift for the 1297 and 1277 cm^{-1} vibrations has been noticed. The calculations predict that the 1207 cm^{-1} vibration can be used as a probe

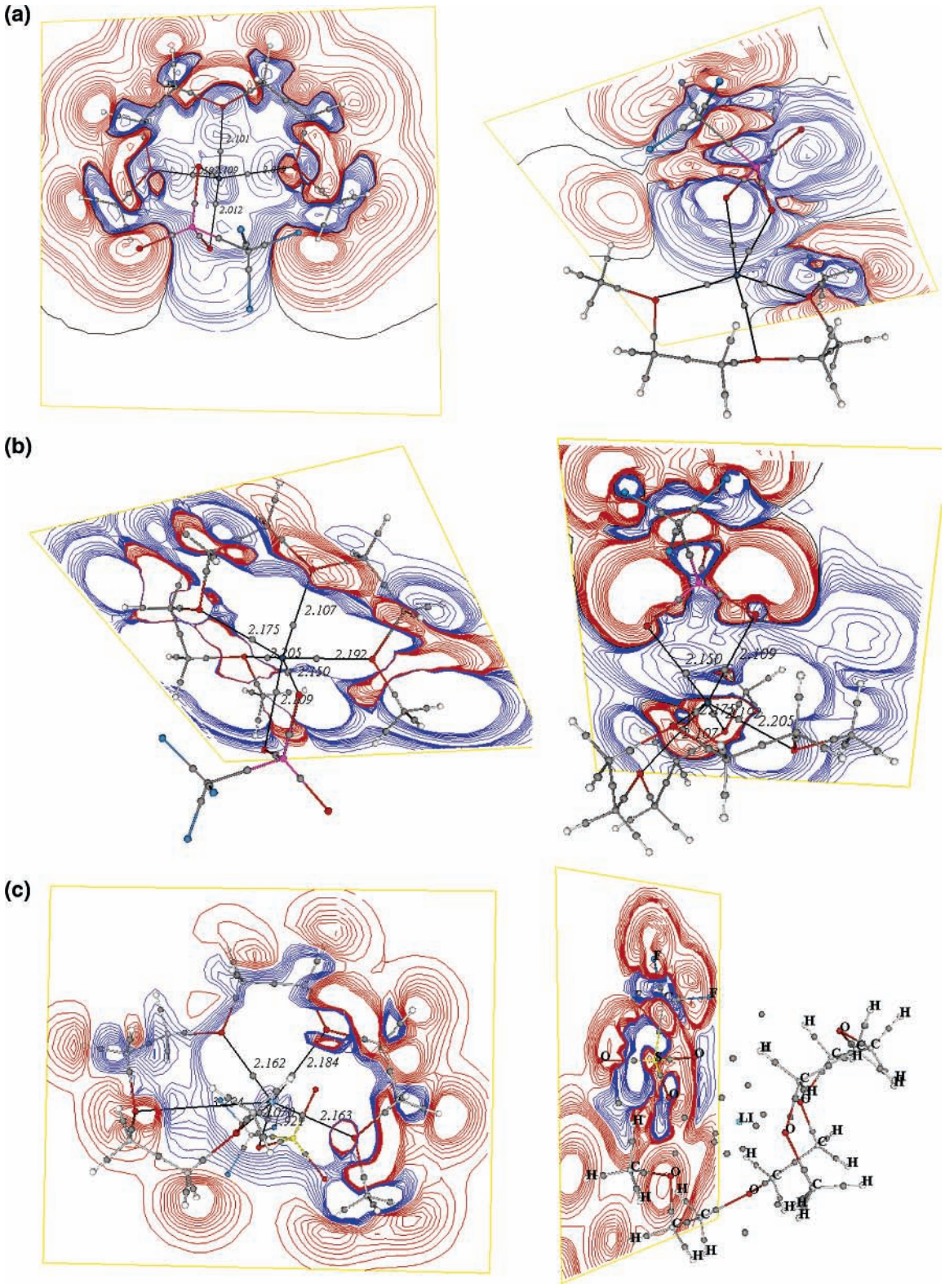

Figure 2. (a) Difference electron density maps in $D_1-Li-CF_3SO_3$ (contours in the range of ±0.001 to ±0.0009 au) are shown. Filled circles in black show the bond critical points. The black line represents a zero valued contour. See text for details. (b) Difference electron density maps in $T_1-Li-CF_3SO_3$ (contours in the range of ±0.001 to ±0.0009 au) are shown. Filled circles in black show the bond critical points. The black line represents a zero valued contour. See text for details. (c) Difference electron density maps in $Te_1-Li-CF_3SO_3$ (contours in the range of ±0.001 to ±0.0009 au) are shown. Filled circles in black show the bond critical points. The black line represents a zero valued contour. See text for details.

to distinguish different metal ion complexes. For example, in the lithium complex, an upshift of 19 cm^{-1} has been predicted whereas its sodium analogue shows a small downshift. This band is not noticed in the triglyme−KTf complex. Tetraglyme−MTf complexes (M = Li, Na, K) can be distinguished by using the 1108 cm^{-1} vibration (CH_2 wag), which leads to a downshift of 6 cm^{-1} in the case of the LiTf complex, whereas a shift in the opposite direction has been noticed for the NaTf complex. For K−Tf, this vibration shows no change in its frequency. (v) Analysis of the anionic vibrations in glyme−MTf complexes

reveals that the change of metal ion from lithium to potassium leads to a downshift of the SO_2 stretching in the anion and follows the rank order: LiTf > NaTf > KTf. A similar trend for the downshift of SO_2 stretching has also been noticed for the metal triflates complexed with the di-, tri-, and tetraglymes. (vi) The contraction of SO and CF bonds (not participating in the ion−ion interactions) in the glyme−M^+Tf^- complexes engenders a blue shift for the corresponding stretching vibrations in the anion. (vii) The downshifts of SO_2 stretching (where the oxygens coordinate to metal triflate) of the anion in the glyme−MTf complexes can be correlated to the strength of the ion−polymer interactions. A large shift (both directions) has been predicted for LiTf−diglyme. These frequency shifts can be rationalized by utilizing the difference electron density maps coupled with the electron density topography and further supported by the NBO analysis.

Acknowledgment. S.P.G. acknowledges support from the Council of Scientific and Industrial Research (Project 01(1772)/02/EMR-II), New Delhi, India.

References and Notes

(1) Johansson, P. *Polymer* **2003**, *48*, 2291.
(2) Johansson, P.; Jacobsson, P. *J. Phys. Chem. A* **2001**, *105*, 8504.
(3) Johansson, P.; Gejji, S. P.; Tegenfeldt, J.; Lindgren, J. *Solid State Ionics* **1996**, *86*−*88*, 297.
(4) Dhumal, N. R.; Gejji, S. P. *Theor. Chem. Acc.* **2006**, *115*, 308.
(5) Dhumal, N. R.; Gejji, S. P. *Chem. Phys.* **2006**, *323*, 595.
(6) Hyan, J.; Dong, H.; Rhodes, C. P.; Frech, R. Wheeler, R. A. *J. Phys. Chem. B* **2001**, *105*, 3329.
(7) Dong. H.; Hyun, J.; Rhodes, C.; Frech, R.; Wheeler, R. A. *J. Phys. Chem. B* **2002**, *102*, 4878.
(8) Johansson, P.; Tegenfeldt, J.; Lindgren, J. *Polymer* **2001**, *42*, 6573.
(9) Gejji, S. P.; Hermansson, K.; Lindgren, J. *J. Phys. Chem. A* **1993**, *97*, 3712.
(10) Huang, W.; Frech, R.; Wheeler, R. A. *J. Phys. Chem.* **1994**, *8*, 100.
(11) Rodes, C. P.; Frech, R. *Macromolecules* **2001**, *34*, 1365.
(12) Frech, R.; Seneviratne, V.; Gadjourova, Z. Bruce, P. *J. Phys. Chem. B* **2003**, *107*, 11255.
(13) Johnston, D. H.; Shriver, D. F. *Inorg. Chem.* **1993**, *32*, 1045.
(14) Johansson, P.; Jacobsson, P. *J. Phys. Chem. A* **2001**, *105*, 8504.
(15) Dhumal, N. R.; Gejji, S. P. *J. Phys. Chem. A* **2006**, *110*, 219.
(16) Dhumal, N. R.; Gejji, S. P. *J. Mol. Struct. (THEOCHEM)* **2006**, *758*, 233.
(17) Rhodes, C. P.; Khan, M.; Frech, R. *J. Phys. Chem. B* **2002**, *106*, 10330.
(18) Becke, D. *J Chem. Phys.* **1993**, *98*, 5684.
(19) Lee, C.; Yang, W.; Parr, R. G. *Phys. Rev. B* **1988**, *37*, 785.
(20) Frisch, M. J.; Trucks, G. W.; Schlegel, H. B.; Scuseria, G. E.; Robb, M. A.; Cheeseman, J. R.; Montgomery, J. A., Jr.; Vreven, T.; Kudin, K. N.; Burant, J. C.; Millam, J. M.; Iyengar, S. S.; Tomasi, J.; Barone, V.; Mennucci, B.; Cossi, M.; Scalmani, G.; Rega, N.; Petersson, G. A.; Nakatsuji, H.; Hada, M.; Ehara, M.; Toyota, K.; Fukuda, R.; Hasegawa, J.; Ishida, M.; Nakajima, T.; Honda, Y.; Kitao, O.; Nakai, H.; Klene, M.; Li, X.; Knox, J. E.; Hratchian, H. P.; Cross, J. B.; Bakken, V.; Adamo, C.; Jaramillo, J.; Gomperts, R.; Stratmann, R. E.; Yazyev, O.; Austin, A. J.; Cammi, R.; Pomelli, C.; Ochterski, J. W.; Ayala, P. Y.; Morokuma, K.; Voth, G. A.; Salvador, P.; Dannenberg, J. J.; Zakrzewski, V. G.; Dapprich, S.; Daniels, A. D.; Strain, M. C.; Farkas, O.; Malick, D. K.; Rabuck, A. D.; Raghavachari, K.; Foresman, J. B.; Ortiz, J. V.; Cui, Q.; Baboul, A. G.; Clifford, S.; Cioslowski, J.; Stefanov, B. B.; Liu, G.; Liashenko, A.; Piskorz, P.; Komaromi, I.; Martin, R. L.; Fox, D. J.; Keith, T.; Al-Laham, M. A.; Peng, C. Y.; Nanayakkara, A.; Challacombe, M.; Gill, P. M. W.; Johnson, B.; Chen, W.; Wong, M. W.; Gonzalez, C.; Pople, J. A. *Gaussian 03*; Gaussian, Inc.: Wallingford, CT, 2004.
(21) Limaye, A. C.; Gadre, S. R. *Curr. Sci. (India)* **2001**, *80*, 1298.
(22) Reed, A. E.; Curtiss, L. A.; Weinhold, F. *Chem. Rev.* **1988**, *88*, 899.
(23) Balanarayan, P.: Gadre, S. R. *J. Chem. Phys.* **2003**, *119*, 5037.
(24) Kearley, G. J.; Johansson, P.; Delaplane, R. G.; Lindgren, J. *Solid State Ionics* **2002**, *147*, 237.
(25) Frech, R.; Seneviratne, V. *Abstracts*; 59th SouthWest Regional Meeting of the American Chemical Society, October 25−28, 2003.
(26) Frech, R.; Rhodes, C. P.; Khan, M. *Macromol. Symp.* **2002**.
(27) Rhodes, C. P.; Frech, R. *Macromolecules* **2001**, *34*, 2660.
(28) Henderson, W. A.; Young, V. G.; Brooks, N. R.; Smyrl, W. H. *Acta Crystallogr. Sect. C: Crys. Struct. Commun.* **2002**, *58*, 201.
(29) Chintapalli, S.; Frech, R. *Electrochim. Acta* **1995**, *40*, 2093.
(30) Rhodes, C. P.; Frech, R. *Solid State Ionics* **2002**, *136*, 1131.
(31) Frech, R.; Chintapalli, S. Bruce, P. G. Vincent, C. A. *Macromolecules* **1999**, *32*, 808.
(32) Frech, R.; Rhodes, C. P. *Solid State Ionics* **2002**, *147*, 259.
(33) Hobza, P.; Havlas, Z. *Chem. Rev.* **2000**, *100*, 4253.
(34) Kock, U.; Popelier, P. L. A. *J. Phys Chem. A* **1995**, *99*, 9747.
(35) Popelier, P. L. A. *J. Phys. Chem. A* **1998**, *102*, 1873.